Self-Assembled Monolayers of Alkanethiols Containing a Polar Aromatic Group: Effects of the Dipole Position on Molecular Packing, Orientation, and Surface Wetting Properties

Stephen D. Evans,† Edward Urankar, Abraham Ulman,* and Nancy Ferris

Contribution from Corporate Research Laboratories and Analytical Technology Division, Eastman Kodak Company, Rochester, New York 14650-2109. *Received August 13, 1990. Revised Manuscript Received February 13, 1991*

Abstract: The effect of incorporating aromatic groups into self-assembled alkanethiol monolayers was studied using a variety of techniques including ellipsometry, wetting, reflection-absorption FTIR, surface (contact) potential, and surface enhanced Raman spectroscopy (SERS). The quality of the monolayers produced was found to be dependent on both the size of the dipole introduced into the film and the length of the aliphatic chain above the aromatic group.

Introduction

The understanding of the interrelationships between the molecular structure of an amphiphile and its organization on different surfaces is of fundamental interest. Indeed, such an understanding at the molecular level is essential for the success of molecular engineering of amphiphiles to produce films with useful properties. An example of interest to us is organic thin films for second-order nonlinear optical applications, where the films should possess a noncentrosymmetric arrangement of molecular dipoles, preferably perpendicular to the substrate surface.[1]

Most amphiphiles with useful second-order nonlinear optical properties contain large π-systems which may be considered to be planar, rigid groups. When such a planar moiety is incorporated into a long alkyl chain, it disrupts the cylindrical symmetry and forms a kink at that position of the chain (Figure 1). Several questions therefore arise: (a) What is the optimal position of the bulky chromophore in the alkyl chain (i.e., closer to the substrate or to the surface)? (b) What are the effects of the total molecular length on the packing and orientation in the two-dimensional assembly? (c) What are the effects of the size (in Å) of the chromophore and the magnitude (in D) of its dipole moment on the packing and orientation of these amphiphiles in the monolayer? These all have to be addressed to ensure the desired control over the order at the molecular level.

By using alkylsulfonyl groups as electron acceptors, one not only obtains the desired high nonlinearity but also has bifunctional chromophores suitable for the incorporation in Langmuir-Blodgett (LB) and self-assembled (SA) films.[2,3] While the fabrication of multilayer films is envisaged to proceed with specific surface reactions, the purification of the trichlorosilane derivatives is by no means a trivial process, and thus a long systematic study would be tedious and difficult.[4-6] Therefore, this study focussed on the use of alkanethiol derivatives as "model" compounds with the hope that the results would lead to the design of suitable molecules for the preparation of SA multilayer films.

In this report, the synthesis and characterization of monolayers formed from molecules of I-VI, Figure 2, in which the chain lengths m and n were varied such that the overall chain length remained constant ($m + n = 16$), is described. This enabled the effect of varying the position of the polar group in an otherwise "fixed" molecule to be studied. To understand the effects of introducing a large dipole moment into the monolayer the sulfone and the sulfide derivatives were compared. The chromophores introduced have dipole moments of ~6.2 D (I-III) and ~2.7 D (IV-VI) (acting in opposite directions), respectively (Figure 2). In addition to molecules I-VI, a derivative of II was prepared in which the alkyl chain connected to the sulfonyl group was perdeuterated, II(D), and a derivative of VI was prepared in which the alkyl chain connected to the sulfide group was mostly perfluorinated, VI(F). The monolayers were subsequently characterized by using ellipsometry, grazing angle FTIR, surface potential, and surface enhanced Raman spectroscopy (SERS) to examine monolayer quality and to estimate molecular orientation. In addition, the surface structure and composition for these monolayers was examined by monitoring the wetting properties of various liquids on these surfaces.

Experimental Section

Substrate Preparation. The substrates employed in this study were prepared by the evaporation of gold (99.999%) onto chromium coated silicon wafers (75 mm × 25 mm). The silicon wafers were cleaned prior to the evaporation by using the following procedure: The silicon wafers were rinsed in millipore water to remove any particulate matter remaining following the scribing of the silicon. They were then ultrasonicated in a mixture of Deconex 12-H_2O (1:10) for 15 min, rinsed, and ultrasonicated with millipore water. The substrates were then either placed in H_2SO_4:H_2O_2 (7:1) at 90 °C for 30 min or plasma etched with a Harrick Plasma cleaner. **Caution!** *A solution of H_2O_2 in H_2SO_4 ("piranha" solution) is a very strong oxidant and reacts violently with many organic materials. It should be handled with extreme care.* The silicon substrates were then rinsed and stored in millipore water until required. The chrome layer evaporated prior to the gold layer was vaporized by resistive heating of a chromium-coated tungsten wire. The deposition rates for the chromium were 1-5 Å per second and the films had typical thicknesses between 75 and 100 Å. The gold films were evaporated from tungsten holders with deposition rates close to 5 Å per second and total thicknesses were typically between 1500 and 2000 Å. The pressure in the vacuum chamber was maintained at 7.5×10^{-6} Torr during the evaporation, using an Edwards turbomolecular pump. The chamber was vented to atmosphere by backfilling it with filtered nitrogen. Surface roughness for substrates employed in this study is p-v 11.00 Å, and RMS 2.40 Å, for the 130 μm length scale. The clean gold surfaces were examined by Auger spectroscopy, and only "normal" carbonaceous-type contamination was found. No chromium was found, indicating that chromium had not diffused from the adhesion layer to the outer surface during the age of the sample (2 weeks). The low-angle X-ray spectrum showed one peak, associated with the (111) face.

Prior to their use the gold substrates were cleaned in the H_2SO_4-H_2O_2 mixture, at 90 °C, for 5 min. The substrates were then rinsed with millipore water and dried in N_2 and their optical constants measured.

Monolayer Preparation. Monolayers were formed by the spontaneous adsorption of the thiols onto gold substrates. In all cases adsorption was carried out from 2×10^{-3} M solutions, using tetrahydrofuran (THF, freshly distilled under N_2 from CaH_2) as the solvent, under N_2. In the studies of the adsorption kinetics, the substrates were removed from solution, washed with THF and absolute ethanol before rinsing thoroughly in millipore water, and dried with N_2. The film thickness was

† Current Address: Department of Physics, University of Leeds, LS2 9JT, United Kingdom.

(1) Prasad, P. N.; Williams, D. J. *Introduction to Nonlinear Optical Effects in Organic Molecules and Polymers*; Wiley: New York, 1990.
(2) Ulman, A.; Willand, C.; Köhler, W.; Robello, D.; Williams, D. J.; Handley, L. *J. Am. Chem. Soc.* **1990**, *112*, 7084.
(3) Tillman, N.; Ulman, A.; Elman, J. F. *Langmuir* **1990**, *6*, 1512.
(4) Tillman, N.; Ulman, A.; Schildkraut, J. S.; Penner, T. L. *J. Am. Chem. Soc.* **1988**, *110*, 6136.
(5) Netzer, L.; Iscovici, R.; Sagiv, J. *Thin Solid Films* **1983**, *99*, 235.
(6) Netzer, L.; Iscovici, R.; Sagiv, J. *Thin Solid Films* **1983**, *100*, 67.

0002-7863/91/1513-4121$02.50/0

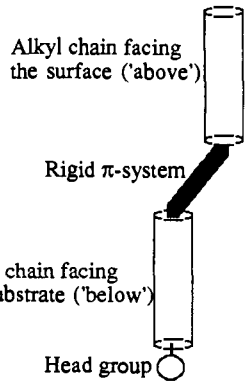

Figure 1. An alkyl chain with a rigid, planar π-system.

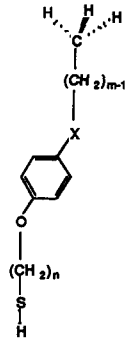

molecule	X	m	n
I	SO_2	4	12
II	SO_2	8	8
III	SO_2	12	4
IV	S	4	12
V	S	8	8
VI	S	12	4
VII	SO_2	11	5

II(D) as II with upper alkyl chain perdeuterated
VI(F) $CF_3(CF_2)_{10}CH_2SC_6H_4O(CH_2)_4SH$

Figure 2. Structures of compounds I–VII.

immediately determined by using ellipsometry (at least 5 readings) and the advancing and receding water contact angles were measured (at least 5 readings). The substrates were then re-immersed in their original solutions and the procedure reiterated.

Monolayer Thickness. The thickness of the monolayers was monitored with use of a Gaertner L116B ellipsometer equipped with a 632.8-nm helium–neon laser. Monolayer thicknesses were determined assuming $n_f = 1.5$, and with the incident and reflected light making a 70° angle to the surface normal. The variation in the measured thickness across the dimensions of any individual sample was ±1 Å.

Wetting Properties. (a) Captive Drop Technique. For cases where advancing and receding angles are reported, measurements were made by forming a droplet on the end of a square cut hypodermic needle and lowering it until the droplet touched the surface. The advancing contact angle was measured when the volume of the droplet was increased *without increasing the solid–liquid interface area.* Similarly the receding angle was the minimum angle measured for a droplet as its volume was reduced *without the solid–liquid interface area changing.*

(b) Free Standing Droplets. For the measurements of hexadecane and the various liquids used for the Zisman plots, readings were taken from free-standing droplets. These were made by forming a droplet at the end of a fine bore capillary tube and lowering it onto the surface. The capillary tube was then removed and the contact angle of the free-standing droplet was measured. All angles were determined with a Ramé-Hart NRL 100 goniometer.

Surface Potential Measurements. The surface potential measurements were carried out by using a Kelvin vibrating electrode arrangement at 25 °C and under a slow flow of nitrogen (the probe surface separation was 0.36 mm). All values are relative to a clean gold substrate and should not be taken as absolute values.

Infrared Measurements. IR measurements of bulk KBr and solution spectra were run on a Perkin-Elmer 1430 spectrometer and have a resolution of ±4 cm^{-1} (the KBr for II(D) was obtained at ±2 cm^{-1}). Grazing-angle (reflection–absorption) FTIR spectra were run on an IBM IR44 spectrometer at a grazing angle of 76°, and peak frequencies are accurate to ±2 cm^{-1}.

Surface Enhanced Raman Spectroscopy (SERS). Sample preparation: Silver metal (Alfa Products 5–9's purity, as received) was thermally deposited onto the previously prepared monolayers. The depositions were performed at a pressure of 7×10^{-6} Torr, and at a rate of 1 Å/s. Rates and mass thicknesses were monitored with an Inficon ATC quartz crystal oscillator. The mass thickness of the deposited silver was approximately 60 Å.

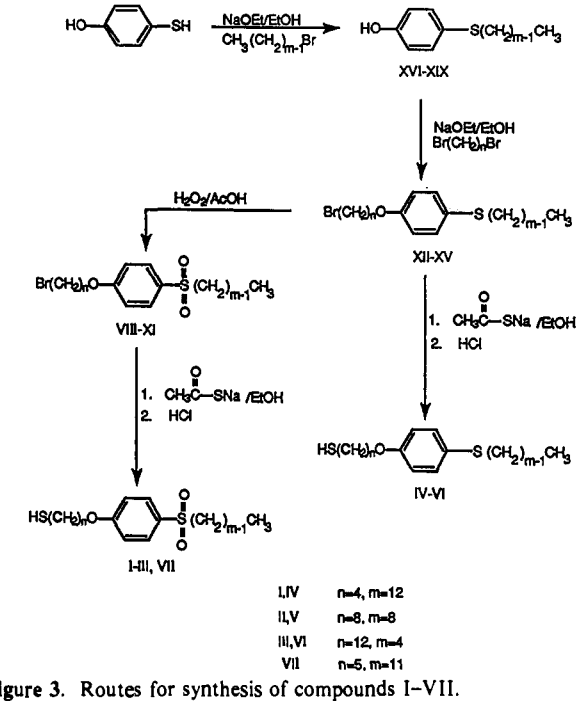

Figure 3. Routes for synthesis of compounds I–VII.

Surface enhanced Raman spectroscopy (SERS): The Raman spectrum for each film was collected with use of 647-nm excitation provided by a Coherent Innova 90-K Kr^+ laser. The samples were held in a stationary position at 60° to the normal. A 90° excitation/collection geometry was employed. The scattered light was collected with a SPEX 1877 Triplemate spectrometer using a 600 groove/mm grating in the dispersive stage and a PAR OMA II/reticon or a Photometrics 512/50 u epi CCD detector system. Additional spectral parameters are noted in the figure captions.

Results

Synthesis. The preparation of molecules I–VI was carried out according to the route shown in Figure 3. It was found that monodeprotonation of 4-mercaptophenol in ethanol containing sodium ethoxide, followed by alkylation of the resulting mercaptide with the appropriate alkyl halide, gives the desired 4-alkylthiophenols (XIV–XIX) in better than 90% yield. These 4-alkylthiophenols were reacted with appropriate 1,ω-dibromoalkanes in ethanol containing sodium ethoxide to yield the corresponding 1-alkylthio-4-(ω-bromoalkyl)benzenes (XII–XV) in moderate yields. The 1-alkylthio-4-(ω-bromoalkyl)benzenes were then converted to the thiols by a reaction adopted from Whitesides et al. in which the bromide is reacted with sodium thiol acetate in ethanol, to give the thiol ester, which gives the desired thiol after trans esterification, catalyzed by concentrated hydrochloric acid (IV–VI).[7] Alternatively, the thioether can be oxidized to the corresponding sulfone with H_2O_2–CH_3COOH (VIII–XI) and then converted to the thiol as described above (I–III, VII). The perdeuterated and perfluorinated materials (II(D), and VI(F), respectively) were also prepared according to these procedures.

Monolayer Formation. Monolayers of molecules I–VI, Figure 2, were formed by immersing gold-coated substrates into the respective 2×10^{-3} M THF solutions, for time periods exceeding 16 h. All monolayers emerged autophobic, i.e., not wet by the solutions from which they were formed. The monolayers were subsequently washed with THF, ethanol, and millipore water and were dried in N_2 prior to their characterization. Table I presents

(7) Bain, C. D.; Troughton, E. B.; Tao, Y.-T.; Evall, J.; Whitesides, G. M.; Nuzzo, R. G. *J. Am. Chem. Soc.* **1989**, *111*, 321.

(8) The rate of monolayer formation is dependent on numerous factors including the solvent type, the solution concentration, the temperature, and the cleanliness of the gold.

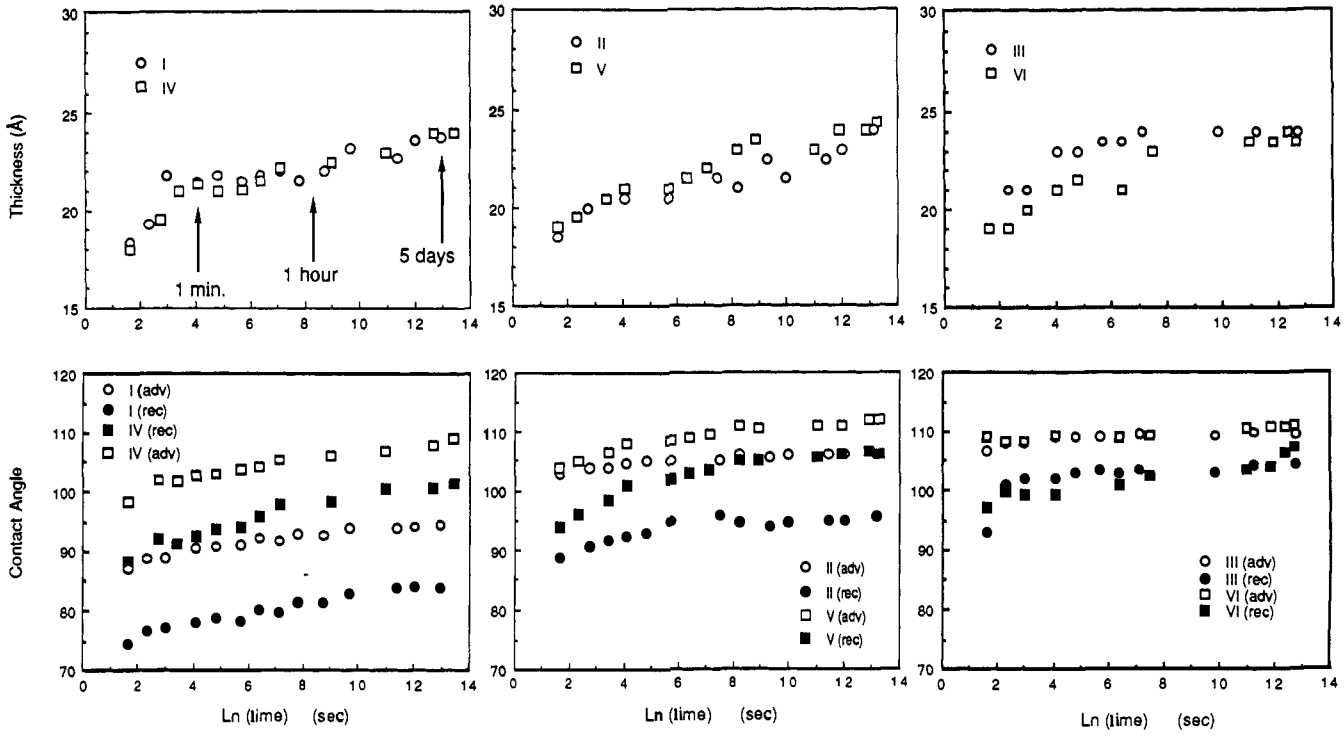

Figure 4. Kinetics of monolayer formation: (a) for molecules of III and VI, (b) for molecules of II and V, and (c) for molecules of I and IV. The sulfones are represented by circles: (●) receding contact angles, θ_r; (○) advancing angles, θ_a. The sulfides are represented by squares (■ for θ_r and □ for θ_a).

Table I. Contact Angles for Thiol Monolayers on Gold[a]

		H_2O[c]		HD[d]	CH_2I_2[d]	thickness,[e]
compd[b]	autophobic	θ_a	θ_r	θ_a	θ_a	±2 Å
I	yes	95	84	35	61	24
II	yes	107	100	43	71	24
II(D)	yes	107	99	45	71	25
III	yes	110	106	45	72	25
IV	yes	109	101	42	64	24
V	yes	112	106	47	69	25
VI	yes	112	107	47	71	25
VI(F)	yes	118	114	76	96	24
VII[f]	yes	107	102	38	63	21

[a] All measurements were made in air at 25 °C. [b] II(D) is the same as molecule II except that the upper C_8 alkyl chain, i.e., above the SO_2 group, is perdeuterated. [c] Measured by the captive drop technique. [d] Measured on free-standing droplets which had been advanced across the surface. [e] Thicknesses estimated with $n_f = 1.5$ for all monolayers except those of VI(F) for which a value of 1.36 was used. [f] VII = CH_3–$(CH_2)_{10}$–SO_2–Ph–O–$(CH_2)_5$–SH.

the average thicknesses obtained for monolayers of molecules I–VII after being left in solution overnight. The values presented are the averages over numerous samples. For any given sample the error in the thickness was ±1 Å and the deviation between samples was ±2 Å.

Kinetics of Adsorption. The kinetics of monolayer formation was studied by monitoring the average monolayer thicknesses (using ellipsometry) and the water contact angles (advancing and receding) as a function of immersion time (Figure 4). Note that film thickness and contact angles are plotted against ln (t), t being the time in seconds. The results reported here are for monolayers adsorbed from 2 mM solutions of THF, at 25 °C, under an ambient of N_2, and onto freshly cleaned hydrophilic gold. There are clearly a large number of parameters which may affect the rate of monolayer formation.[9] However, it was found that adsorption kinetics were similar for molecules in which the positions of the aromatic groups in the chains were the same, i.e., for I & IV, II & V and III & VI, with the largest difference being between I & IV and III & VI. For monolayers of III & VI there were no observable changes in the wetting or thickness after an hour. On the other hand, it took several days before complete monolayers of I & IV were formed. Thus, under the conditions given above, the rate of adsorption is dependent on the length of the *alkyl chain above the aromatic group* (rate of monolayer formation III, VI > II, V > I, IV). The addition of a large dipole does not appear to adversely affect the kinetics of adsorption for these monolayers. The perfluorinated version of VI, VI(F), displayed extremely fast monolayer formation which may be attributed to the rigidity, and hence fewer degrees of freedom, associated with the perfluorinated portion of the upper alkyl chain.

Contact Angle Measurements. The wetting properties of the monolayers were determined by measuring the contact angles of water, methylene iodide (CH_2I_2, MI), and *n*-hexadecane ($C_{16}H_{34}$, HD). The surface free energy, γ_{lv}, values for water, MI, and HD are 72.8 ($\gamma^p = 51$, $\gamma^d = 21.8$), 50.8 ($\gamma^p = 0.38$, $\gamma^d = 50.42$), and 27.6 ($\gamma^d = 27.6$, $\gamma^p = 0$), respectively. The values given in parentheses correspond to the polar (γ^p) and dispersive (γ^d) components of the surface free energy.[9-11] Due to the continuing debate on whether the Neumann equation of state is valid or not (and hence conversely as to whether the splitting of the surface free energy into polar and nonpolar components has any meaning) both approaches for estimating the surface energy are used side by side.[12-14] It was hoped that if such polar and dispersive components had any physical significance they would be manifested in the case of the sulfones, for which the polar interactions were expected to be much larger than for the sulfides. It was also of interest to see how these components varied as a function of depth, i.e., of the distance of the polar group from the mono-

(9) Janczuk, B.; Bialopiotrowicz, T. *J. Colloid Int. Sci.* **1989**, *127*, 59.
(10) Janczuk, B.; Bialopiotrowicz, T.; Wojcik, W. *J. Colloid Int. Sci.* **1989**, *127*, 189.
(11) The Neumann equation of state approach sees no validity to the splitting of the surface free energy into polar and dispersive parts as is often quoted in the literature and it does not allow the determination of these components from contact angle measurements. In particular it recognizes the components calculated in such a fashion to be no more than "...adjustable parameters which are functions of the total surface tensions γ_s and γ_l".
(12) Neumann, A. W.; Good, R. J.; Hope, C. J.; Sepal, M. *J. Colloid Int. Sci.* **1974**, *49*, 291.
(13) Spelt, J. K.; Neumann, A. W. *Langmuir* **1987**, *3*, 588.
(14) Spelt, J. K.; Absolom, D. R.; Neumann, A. W. *Langmuir* **1986**, *2*, 620.

Table II. Critical Surface Tensions for Thiol Monolayers on Gold[a-c]

compd	γ_c	γ_{sv}	γ_s^p	γ_s^d	$\gamma_{sv}^{E.S.}$	ref
I	21	25.2	2.3	22.8	22.9	this work
II	21	21	0.4	20.6	20.9	this work
II(D)	21	20.5	0.5	20	20.9	this work
III	19	20.3	0.2	20.1	20.4	this work
IV	21.5	21.1	0.3	20.8	21.2	this work
V	20	19.2	0.0	19.2	19.8	this work
VI	19	19.5	0.1	19.4	19.8	this work
VI(F)	9	10.9	0.3	10.6	11.3	this work
$CF_3(CF_2)_{10}CO_2H/Pt$	6					12
PTFE	18					13
$CH_3(CH_2)_{21}SH/Au$	19					3

[a] All measurements were made at 25 °C in air. The values are given in units of mN m^{-1}. [b] The values of γ_{sv} were calculated by using the water and hexadecane contact angles. [c] $\gamma_{sv}^{E.S.}$ represents the values of γ_{sv} calculated from the hexadecane contact angles (given in Table I) and the reformulated equation of state given by Li and Neumann, to be published. It was noted that widely varying values of γ_{sv}, for any given surface, are obtained depending upon which liquid is being used. It is also noted that such variations also occur when the modified Fowkes-type equation is used.

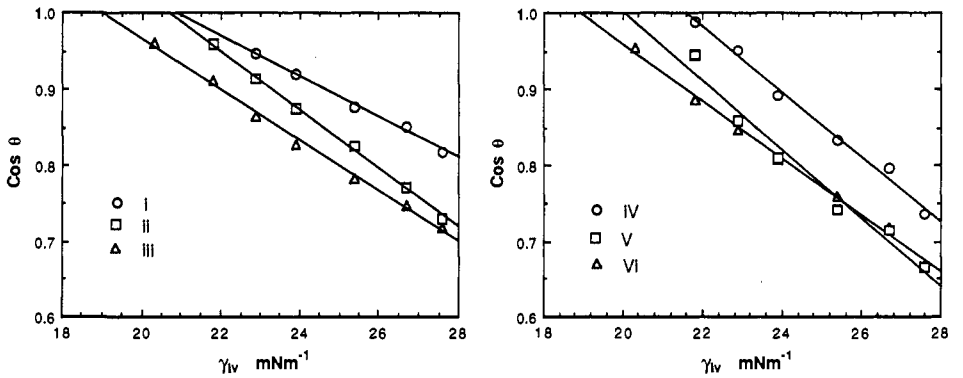

Figure 5. Zisman plots for monolayers of I–VI (constructed by using a series of *n*-alkanes).

layer–air interface. Hexadecane, which interacts through dispersive forces only, is thought to be much more sensitive to the structure at the monolayer–air interface and it was hoped the HD contact angles would yield information regarding the "quality" and composition of the monolayer surfaces. The results reported in Table I show several interesting features. Considering the sulfones only (I–III), one sees that the contact angles of all three liquids show the same general trend in that their values diminish as one moves through the series, such that $\theta_{III} > \theta_{II} > \theta_I$ *for any given liquid*. The size of the variation for the total change in water contact angle was $\Delta\theta \approx 15°$, while for HD and MI $\Delta\theta \approx 10°$. In addition, the hysteresis of the water contact angle ($\theta_{adv}-\theta_{rec}$) increased from ~5° to ~10°. Such variations may be associated with either an increase in disorder at the monolayer–air interface as the chromophore is brought closer to the surface or to increasing polar interactions between chromophore and the liquid droplet, or both. The sulfides IV–VI showed a similar trend with $\theta_{VI} > \theta_V > \theta_{IV}$ for the various liquids; however, the size of the changes was much smaller than that observed for the sulfones. The total change in water contact angle was $\Delta\theta \approx 3°$, while for HD and MI $\Delta\theta \approx 5°$ and 7°, respectively. In general, comparing the sulfides to their respective sulfones, the sulfides give higher contact angle values, which is consistent with either lower polar interactions between the monolayer and the probing liquid or to less disorder at the surface of the sulfide monolayers.

All the contact angle values reported, with the possible exception of those found on monolayers of I, are consistent with the picture of having close-packed methyl-terminated surfaces.[15-17]

Critical Surface Tensions. Table II presents the critical surface tensions for the monolayers studied here and, for comparative purposes, some relevant literature values. The values presented here were estimated from linar extrapolations of cos (θ_a) vs γ_{lv} for a series of *n*-alkanes (Figure 5). The correlation functions for these fits were close to unity (in all cases better than 0.99).

Table III. Surface Potential of Monolayers[a]

compd	surface potential with respect to bare gold, mV	apparent dipole moment, $\mu_\perp$,[b] D
I	242 ± 50	0.36
II	195 ± 11	0.29
III	64 ± 6	0.09
IV	310 ± 31	0.46
V	323 ± 43	0.48
VI	466 ± 20	0.69
VI(F)	−750 ± 46	−1.12
DDT	600 ± 30	0.89

[a] Surface potentials were measured in light, at 25 °C, under a slow flow of N_2. [b] Assuming the dielectric constant is that for bulk polyethylene, i.e., $\epsilon = 2.25$. 1 D = 3.335×10^{-30} C.

In keeping with the wetting results described above it was found that the critical surface tensions were lowest for monolayers formed from molecules of III and VI, where the bulky groups are farthest from the monolayer–air interface. The values of 19 mN m^{-1} for these surfaces are comparable to the lowest values reported for alkane thiols adsorbed onto gold substrates.[7] The γ_c values increased to around 20 mN m^{-1} for the monolayers of V, and to around 21 mN m^{-1} for monolayers of I, II, and IV. All of these values are consistent with surfaces composed of methyl-terminated alkyl chains, which when considering the shortness of the "upper" alkyl chains involved gives surprisingly low values for the critical surface tension. Monolayers formed from VI(F) gave very low γ_c values, ca. 9 mN m^{-1}, which although not as low as the value of 6 mN m^{-1} reported by Hare et al.[18] for $CF_3-(CF_2)_{10}-CO_2H$ on platinum are much lower than the value of 18 mN m^{-1} found for PTFE surfaces and are therefore believed to be indicative of a surface comprised mainly of CF_3 groups.

Surface Potential Measurements. The surface potential (contact potential difference) of monolayers was measured with respect to a reference electrode by using the Kelvin "vibrating probe"

(15) Ray, B. R.; Bartell, F. E. *Colloid Sci.* **1953**, *8*, 214.
(16) Adam, N. K.; Elliott, G. E. P. *J. Chem. Soc.* **1962**, 2206.
(17) Fox, H. W.; Zisman, W. A. *J. Colloid Sci.* **1952**, *7*, 428.
(18) Hare, E. F.; Shafrin, E. G.; Zisman, W. A. *J. Phys. Chem.* **1954**, *58*, 236.

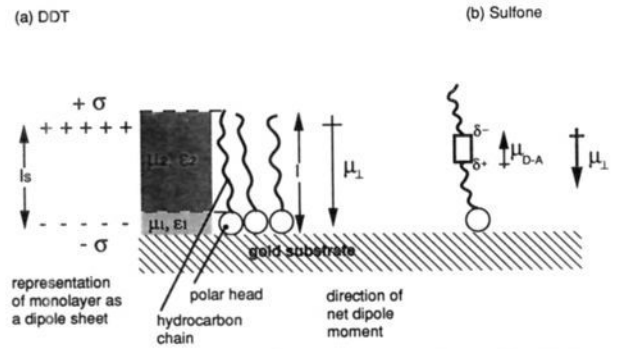

Figure 6. The representation of a monolayer as a charged double layer: (a) for a monolayer of a straight chain alkylthiol and (b) for a monolayer of molecules with donor–acceptor groups. The convention used here depicts dipole moments as acting from + to −, i.e., in the direction of the electric field.

technique.[19-22] Table III presents the results obtained for monolayers of I–VI and for comparison purposes values obtained for the partially perfluorinated version of VI and for DDT (dodecanethiol, CH_3–$(CH_2)_{11}$–SH). The values quoted are the averages of many readings taken from several samples.

There are two points of interest. First, the sign of the potential step and second the magnitude of the variation. Before considering molecules I–VI an explanation of the results found for a monolayer of DDT is presented, which is then extended for the other monolayers under study. For simplicity, the DDT is considered to be in an all-trans configuration and nearly perpendicular to the surface. It is generally thought that the thiol hydrogen is lost on chemisorption, resulting in a Au–S interaction.[23] If this interaction is of a polar nature (e.g., $Au^{\delta+}$–$S^{\delta-}$) then this bond will have a net dipole moment with a permanent component perpendicular to the surface. The monolayer could thus be visualized as a "tightly-bound" dipole sheet at the metal surface. Electrons trying to move out of the metal would "see" this sheet as a potential barrier (electrostatic) which leads to an *increase* in the work function and hence a *decrease* in the observed surface potential. If the work function of the vibrating electrode is ϕ_a, and ϕ_b is that of the bare gold reference sample, then the contact potential difference (surface potential) for the reference sample is given by

$$\phi_a - \phi_b = U_{ref} \tag{1}$$

The monolayer "modified" surface (with work function ϕ_b') is given by

$$\phi_a - \phi_b' = U_{mon} \tag{2}$$

Subtracting eq 1 from eq 2 simply yields

$$\phi_b - \phi_b' = U_{mon} - U_{ref} = \Delta U \tag{3}$$

The observed positive change in $U_{mon} - U_{ref}$, ΔU, for monolayers of DDT, implies that the work function ϕ_b' decreases and hence implies that the surface dipole layer is oriented such that a sheet of negative charges resides close to the metal surface and a sheet of positive charges lies further away toward the monolayer-ambient interface (Figure 6a). Thus, it is not possible for the Au–S bond to be the dominant dipole contribution.[24]

The surface potential can be written in terms of the net perpendicular component of the molecular dipole moment[25-27]

$$\Delta U = \mu_\perp l/\epsilon\epsilon_0 V_m = \mu_\perp/\epsilon\epsilon_0 A \tag{4}$$

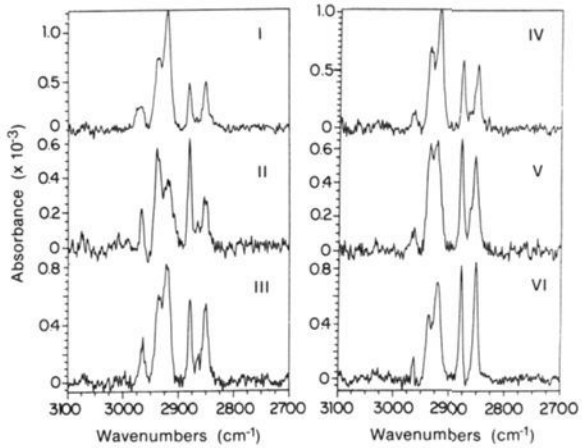

Figure 7. IR reflection–absorption spectra showing the "high-frequency" CH_2 and CH_3 stretch regions for monolayers of I–VI.

where A is the area per molecule, ϵ the relative permittivity of the monolayer, and ϵ_0 the permittivity of free space.[28] Hence, for DDT, taking $\epsilon = 2.25$, eq 4 gives $\mu_\perp = 0.896$ D.[29]

In the case of monolayers of I–VI, one would expect the incorporation of the polar chromophore to have a significant effect on the measured surface potential. Since the orientation and packing density of the molecules in these films is likely to be different from those in regular alkanethiol monolayers (e.g., DDT), one cannot *quantitatively* compare the results for these different monolayer systems. However, considering sulfones I–III, it is expected that the dipole associated with the chromophore will act to *oppose* that found in the same molecule if the dipole associated with the chromophore was zero. This can be understood better if the net dipole $\mu_\perp$ is considered to be composed of two components $\mu_{DA\perp}$ and $\mu_{RES\perp}$ where $\mu_{DA\perp}$ is the perpendicular component of the dipole associated with the donor–acceptor group and $\mu_{RES\perp}$ is the residual perpendicular component of the dipole moment that the molecules would exhibit if $\mu_{DA\perp} = 0$ (Figure 6b). From the results of our previous study on surface potential of regular alkanethiol monolayers on gold (and that shown above for DDT), it is reasonable to assume that $\mu_{RES\perp}$ should be positive, i.e., acting in the direction shown in Figure 6a.[24] Since $\mu_{DA\perp}$ acts in the *opposite* direction to $\mu_{RES\perp}$ one can write

$$\mu_\perp = \mu_{RES\perp} - \mu_{DA\perp} \tag{5}$$

This implies that $\mu_\perp$ should be smaller than $\mu_{RES\perp}$ and possibly negative. From Table III one can see that $\mu_\perp$ is close to zero for monolayers of III indicating that $\mu_{RES\perp}$ and $\mu_{DA\perp}$ are approximately of equal magnitude. However, as the position of the chromophore in the molecules is varied, it is seen, rather unexpectedly, that the magnitude of the apparent dipole, $\mu_\perp$, also changes.

For the sulfides, the dipole associated with the chromophore $\mu_{DA\perp}$ acts in the *same* direction as $\mu_{RES\perp}$ and hence yields

$$\mu_\perp = \mu_{RES\perp} + \mu_{DA\perp} \tag{6}$$

Therefore for these monolayers, $\mu_\perp$ should be greater than $\mu_{RES\perp}$ and must be positive. If $\mu_{RES\perp}$ is the same for both the sulfones and the sulfides then one can also say that $\mu_\perp$ for the sulfides should be greater than $\mu_\perp$ for the sulfones. Indeed, it was found that the $\mu_\perp$ values for the sulfides were greater than those for the sulfones. The variation of $\mu_\perp$ with the position of the chromophore was again noted and will be returned to in the Discussion section.

(19) Lord Kelvin *Philos. Mag.* **1989**, *46*, 82.
(20) Davies, J. T.; Rideal, E. K. *Interfacial Phenomena*; Academic Press: New York, 1961.
(21) Gaines, G. L., Jr. *Insoluble Monolayers at Liquid–Gas Interfaces*; Interscience: New York, 1966.
(22) Adamson, A. W. *Physical Chemistry of Surfaces*; Wiley: New York, 1982.
(23) Laibinis, P.; Whitesides, G. *Langmuir* **1990**, *6*, 87.
(24) Evans, S. D.; Ulman, A. *Chem. Phys. Lett.* **1990**, *170*, 462.
(25) Demchak, R. J.; Fort, T., Jr. *J. Colloid Int. Sci.* **1974**, *46*, 191.
(26) Vogel, V.; Möbius, D. *Thin Solid Films* **1988**, *159*, 73.
(27) Oliveira, O., Jr.; Taylor, D. M.; Lewis, T. J.; Salvagno, S.; Stirling, J. M. *J. Chem. Soc., Faraday Trans. I* **1989**, *85*, 1009.
(28) The effects of mutual interactions between adsorbed molecules (i.e., depolarization effects) have been neglected in the derivation of eq 6. For such effects to be taken into account an additional term would need to be included in eq 5 which would make allowances for induced dipole effects; such a term would necessarily be dependent on the polarizability of the molecules.
(29) For free thiols $\mu \approx 1.5$ D (McClellan, A. L. *Tables of Experimental Dipole Moments*; W. H. Freeman & Company: San Francisco, 1963).

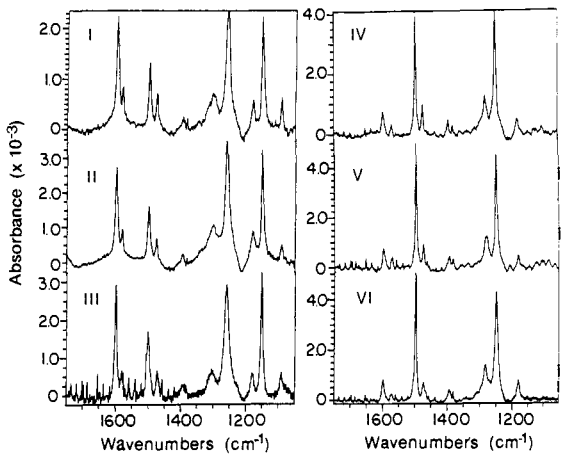

Figure 8. IR reflection–absorption spectra showing the "mid-frequency" region, 1750–1050 cm^{-1}.

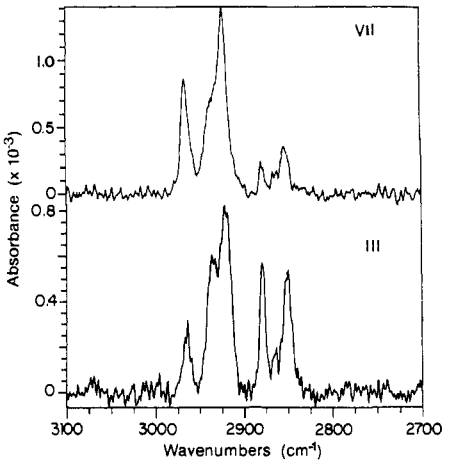

Figure 9. Monolayer spectra, illustrating the effect of displacing the aromatic group by one carbon. The upper and lower traces show the grazing-angle spectra for the monolayers of CH_3–$(CH_2)_{10}$–SO_2–Ph–O–$(CH_2)_5$–SH and CH_3–$(CH_2)_{11}$–SO_2–Ph–O–$(CH_2)_4$–SH, respectively.

The perfluorinated monolayers gave large negative changes in surface potential (ca. −750 mV) which is due to the strong electron-withdrawing properties of the fluorine atoms. For these monolayers the net dipole thus acts in the opposite direction than found for the other monolayers.

Infrared Characterization. Figures 7 and 8 display the reflection–absorption (grazing-angle) spectra found for monolayers of I–VI for the high-frequency (CH_2, CH_3) region and the mid-frequency region, respectively. From Figure 7 it is apparent that all the spectra are essentially similar to those found for straight-chain alkanethiols adsorbed on gold.[30] The "high-frequency" region yields information on the "crystalline-like" nature of the monolayers. However, for the monolayers studied here, ambiguities are introduced into the interpretation of the CH_2-stretches, since these have contributions from the hydrocarbon portions above and below the aromatic group, and it is not necessary for these to be the same. In an attempt to separate the different contributions (and hence the ordering in the upper and lower portions of the molecule), a perdeuterated version of II, II(D), was made in which the upper alkyl chain was entirely perdeuterated. The CD_2 and CD_3 vibrations, between 2000 and 2300 cm^{-1}, are less well resolved and are of lower intensity that the CH_2- and CH_3-stretches. It was found that the C–D peaks in the monolayer were shifted by approximately 10 cm^{-1} to higher energy than those calculated from the bulk spectra. We attribute the stretches circa 2220 and 2097 cm^{-1} to the CD_2 asymmetric and symmetric vibrations, respectively.[31]

The mid-frequency region contains most of the information regarding the phenyl vibrations and those of the donor and acceptor substituents. The sulfides IV–VI (Figure 8) show four clear phenyl vibrations between 1600 and 1470 cm^{-1}. These are typical of a para-substituted phenyl group, with weak vibrations at 1600 cm^{-1} (C_{2v}, a_1) and 1575 cm^{-1} (C_{2v}, b_2), a strong vibration at ca. 1500 cm^{-1} (C_{2v}, a_1), and a weak vibration close to 1475 cm^{-1} (C_{2v}, b_2). The a_1 species of vibrations are parallel to the principal axis of the phenyl group, while the b_2 species are perpendicular to it. The aryl oxygen stretch, below the ring, has a characteristic frequency close to 1250 cm^{-1}. For the sulfones I–III (Figure 8), the SO_2 group has a strong effect on the phenyl spectra due to its electron-withdrawing properties, which when coupled with the electron donor below the ring leads to an enhanced conjugation of the ring. This increase in the effective conjugation leads to a marked intensification of the 1600 and 1580-cm^{-1} vibrations. For the sulfones, the aryl–oxygen stretch is shifted to higher energies by ~10 cm^{-1} due to the interaction of the oxygen electrons with the delocalized π-electrons of the phenyl, as expected from the changes in intensity of the 1600-cm^{-1} vibrations. The symmetric sulfone stretch appears strong, at around 1150 cm^{-1}, which is approximately 5 cm^{-1} higher than that for the corresponding KBr samples and nearly 10 cm^{-1} higher than that found for the solution spectra; its asymmetric counterpart, however, is not easily assigned in the monolayer spectra, through there is evidence in some spectra that it may occur between 1310 and 1320 cm^{-1}. The most probable cause for its low intensity is that the $\nu_{as}(SO_2)$ stretch is in the plane in the film and is therefore precluded by the surface selection rules.[32] The bulk spectra, both $CHCl_3$ and KBr, clearly show the $\nu_{as}(SO_2)$ stretch at ca. 1318 cm^{-1}. A further band, found only in the sulfone spectra, was that of a strong absorption at around 600 cm^{-1} which has been tentatively ascribed to the SO_2 scissor deformation.[33]

Figure 9 shows the effect of moving the position of the aromatic group in the chain by one carbon (i.e., for a $CH_3(CH_2)_{10}$–SO_2–Ph–O–$(CH)_5$–SH) in comparison to that obtained from monolayers of III. The main spectral differences occur in the high-frequency region of the IR and are indicative of the different surfaces produced.

Attempts to gain some information about the orientation of the molecules in the monolayers were made following the approach described by Allara et al. of comparing the monolayer spectra to those obtained from calculations for a randomly distributed overlayer of the same thickness.[34–38] If there are no differences in the spectra due to the binding of the monolayer to the gold surface, then the differences which do occur between the spectra may be interpreted as being due to differences in the orientation of the molecules in the two films. Calculations were made for two of the compounds, II(D) and III. The material constants were determined from bulk KBr spectra by using an iterative procedure which involved a Kramers–Kronig transform and a calculation of the bulk spectra using the Fresnel transmission coefficients for a three-phase model. Four iterations were found to give acceptable convergence between the KBr and the calculated bulk spectra. The reflection spectra for isotropic 24-Å thick films were then computed for the various spectral regions for a 76° grazing angle and with the following values for the refractive indices of the gold; $n = 1$, $k = 29$ for the region 3100–2700 cm^{-1}; $n = 2$, $k = 39$ for

(30) Porter, M. D.; Bright, T. B.; Allara, D. L.; Chidsey, C. F. D. *J. Am. Chem. Soc.* **1987**, *109*, 3559.

(31) The bands were determined from comparisons between the integrated peak areas of the bulk and monolayer spectra. We note that these peak assignments differ from those of Mowery and Dote, see below, and we have a paper in preparation, on a different monolayer system, which supports our present speculation. Mowery, R. L.; Dote, J. L. *Mikrochim. Acta* [*Wien*] **1988**, *11*, 69.

(32) Greenler, R. G. *J. Chem. Phys.* **1966**, *44*, 310.

(33) Bentley, F. F.; Smithson, L. D.; Rozek, A. L. *Infrared Spectra and Characteristic Frequencies* ~700–300 cm^{-1} **1968**, 79–80.

(34) Allara, D. L.; Swalen, J. D. *J. Phys. Chem.* **1982**, *86*, 2700.

(35) Allara, D. L.; Nuzzo, R. G. *Langmuir* **1985**, *1*, 52.

(36) Nuzzo, R. G.; Fusco, F. A.; Allara, D. L. *J. Am. Chem. Soc.* **1987**, *109*, 2358.

(37) Allara, D. L.; Baca, A.; Pryde, C. A. *Macromolecules* **1978**, *11*, 1215.

(38) Nuzzo, R. G.; Dubois, L. H.; Allara, D. L. *J. Am. Chem. Soc.* **1990**, *112*, 558.

Table IV. Orientation of C-H and C-D Modes for Monolayers of II(D) and III[a]

	mode	I_{obs}	I_{cal}	$I_{obs}/3I_{cal}$	θ
II(D)	$\nu_{as}(CH_2)$	5.8	5.9	0.3	57
	$\nu_s(CH_2)$	3.0	3.6	0.3	57
	$\nu_{as}(CD_2)$	3.3	3.6	0.3	57
	$\nu_s(CD_2)$	2.0	3.0	0.2	63
III	$\nu_{as}(CH_2)$	8.0	14.0	0.2	63
	$\nu_s(CH_2)$	5.5	8.3	0.2	63

[a] The angle the transition moment makes with the surface normal, θ, is determined by using $\cos^2\theta = I_{obs}/3I_{cal}$. From the values for $I_{obs}/3I_{cal}$ one can obtain values for the average tilt, α, and twist, β, of the C-D and C-H chains. For II(D) these results yield, for the perdeuterated chain, $\alpha = 47°$ and $\beta = 50°$, and for the protonated chain $\alpha = 51°$ and $\beta = 57°$. For monolayers of III the upper and lower portions of the molecule cannot be distinguished and hence the values represent an average of both portions, $\alpha = 40°$ and $\beta = 43°$.

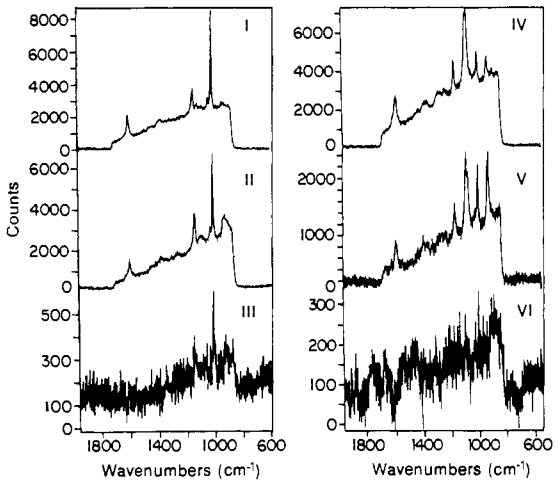

Figure 10. SERS of sulfone and sulfide monolayers. Spectral collection parameters: $\lambda_{ex} = 647$ nm, laser power = 50 mW at sample, 4-cm^{-1} slits, 2 min total integration per spectrum, detector system PAR OMA II/reticon.

the region 2400–1900 cm^{-1}; and $n = 4$, $k = 50$ for the region 1750–1050 cm^{-1}.[39] The values of $I_{obs}/3I_{cal}$ (see refs 34–38 for more details) are given in Table IV, where I_{obs} is the intensity of the monolayer spectra for a given mode and I_{cal} is the calculated reflection intensity for the same mode. These values yield the tilt angles, α, and rotations about the molecular axis, β, for the various modes considered.[34-38] For molecules of II(D) the orientation of the CH_2 and CD_2 chains can be calculated independently to yield information on the upper and lower portions of the monolayer. A more detailed analysis of the results is given in the Discussion section.

Surface Enhanced Raman Spectroscopy (SERS). The SERS experiments described here follow those described originally for self-assembled monolayers by Kim et al.[40] Figure 10 presents the SERS in the mid-frequency region for the six monolayers studied. The spectra of the monolayers formed from the sulfonyl compounds exhibited strong bands associated with the aromatic ring structure (~1000 and ~1600 cm^{-1}) and with the SO_2 group (1140 cm^{-1}). The relative intensities of the bands in the SERS differ considerably from the normal Raman intensities observed for the bulk materials. In addition to these selective band enhancements, we also observe an overall decrease in the scattering intensity as the aliphatic tail is lengthened from four carbons to twelve carbons.

The band, which is observed most strongly in the SERS of the sulfide monolayers, occurs at ~1080 cm^{-1}. In addition to this

(39) Ordal, M. A.; Long, L. L.; Bell, R. J.; Bell, S. E.; Bell, R. R.; Alexander, R. W.; Ward, C. A. *Appl. Opt.* **1983**, *22*, 1099–1119.
(40) Kim, J.-H.; Cotton, T. M.; Uphaus, R. A. *Thin Solid Films* **1988**, *160*, 389.

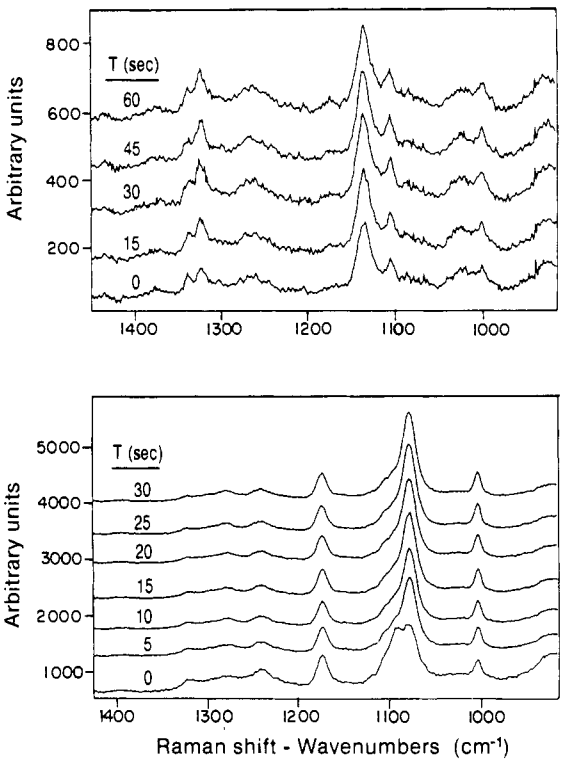

Figure 11. SERS spectra of C_8 monolayers as a function of exposure/collection times: (a) C_8SO_2, (b) C_8S. Spectral collection parameters: $\lambda_{ex} = 647$ nm, laser power = 125 mW at sample, 4-cm^{-1} slits, integration times noted for each trace, detector system Photometrics 512/50 u epi CCD.

feature, bands are also observed near 1000 and 1600 cm^{-1}. During the course of the experiments, we observed some dependence of the sulfide monolayer spectrum on incident power levels. Figure 11 presents the results of a series of spectral scans at a single incident power as a function of time for both the C_8S monolayer (V) and the C_8SO_2 monolayer (II). For the C_8SO_2 film, the spectrum appears stable over the course of the data collection (total time 75 s with spectra collected at 15-s intervals). In contrast, the spectrum of the C_8S film changes with the time of exposure to the incident laser radiation (total time 35 s with the spectra collected at 5-s intervals). The peak at 1092 cm^{-1} rapidly loses intensity and the band at 1078 cm^{-1} becomes stronger over the course of 35 s. In fact, the spectrum of the C_8S monolayer after 35 s of exposure is similar to the spectrum of the C_8S monolayer in Figure 10 which represents a 2 min total integration time of the signal.

Discussion

From the kinetics of adsorption it was found that monolayers of III & VI were more or less complete, as determined by their thickness and water contact angles, after approximately 1 h. The rate of monolayer formation was strongly dependent on the position of the chromophore within the alkyl chain. Molecules that had their longer alkyl-chain portions *above* the chromophore (i.e., *closer* to the monolayer–air interface) formed monolayers faster than those that had them below. It can therefore be suggested that the length of the upper alkyl chain provides a strong driving force for monolayer formation by maximizing the van der Waals interactions. However, this cannot be the only driving force, since films of the appropriate thickness and with high water contact angles are formed from the other materials studied, even those with the short $m = 4$ chains above the chromophore (all monolayers gave final thicknesses of 24 ± 2 Å). From CPK model calculations it is estimated that these monolayers should exhibit a thickness of 27.5 Å, assuming that they are comprised of molecules with all-trans alkyl chains and with the chain axes normal to the substrate surface. The molecules under study here may be considered to be composed of three segments: the upper

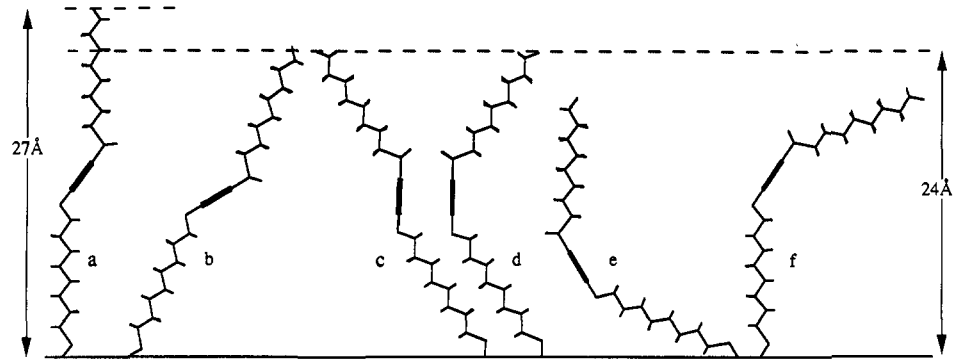

Figure 12. Possible monolayer configurations for molecules of II.

alkyl chain, the lower alkyl chain, and the phenyl ring. Even in the simplest treatment of this case (where all portions are considered to be rigid rods, and with rotation about the phenyl–SO_2 bond and phenyl–O bond being the only allowed degrees of freedom), there are many possible molecular orientations that could account for the observations made here. Figure 12 shows six conformation possibilities (the molecular orientations have been restricted to being in the plane of the page) which seem likely contenders, obviously there are more. It is important to note, however, that while there has been an impressive advancement in the analytical tools available for studies of the kind reported here, we still lack microscopic evidence for the suggested molecular structures, because of the average nature of our measurements. We may get an idea of the *average* microscopic structure of molecular assemblies from detailed molecular dynamics simulations (MD),[41] the results of which are to be published in a separate report.[42] However, in this case we are faced with the dilemma that the results are as good as the force field used, and at present, a full understanding of how to add atomic charges to the molecules under study is not at hand. In the following discussion efforts will be made to rule out the most unlikely structures, and it is noted that it is improbable that there will be a single molecular orientation within these films.

In the first case (Figure 12a), the overlayer may be envisaged as being composed of molecules in an anti configuration oriented perpendicular to the substrate surface but with a fractional coverage. From the ellipsometric results found here this would correspond to an approximate coverage close to 90%.[43] Cases *b* and *c* in Figure 12 correspond to monolayers composed of molecules, again in anti configurations, but which are oriented so that the molecular axis along the carbon backbone makes an angle of 30 ± 5° to the surface normal; these correspond to a rotation of *a* by ±30°. Note that these cases have quite different implications for the orientation of the phenyl ring and the terminal CH_3 groups. If there is a 180° rotation about the phenyl–SO_2 bond (or about the phenyl–O bond), then the molecule would be in a syn form. Cases *d*–*f* in Figure 12 show several variations of this form; however, only case *d* is consistent with the ellipsometry (this would not be the case for molecules of I, III, IV, and VI where *e* and *f* may also be correct). In attempting to understand the molecular orientation in the C_8 systems, cases *e* and *f* can be ruled out immediately on the basis of ellipsometry.

The difference in the adsorption rates of the long (m = 12) and short (m = 4) thiol derivatives may result from differences in conformational order between the alkyl chains above and below the phenyl moiety. Preliminary MD runs on I–VI and a complete 200 psc MD run on II suggest that the alkyl chains below the chromophore are more disordered than those above it. This is because when the thiol molecule adsorbs on the surface it is not in the all-trans configuration, but rather has gauche bonds and kinks along its alkyl chains. The number of gauche bonds is related linearly to the number of methylene units in the chain, i.e., there are more gauche bonds in a C_{12} alkyl than in a C_4 one. While the alkyl chain above the chromophore can easily rotate to the all-trans configuration, the one below the chromophore is pinned at both ends (to the surface and to the chromophore). Hence, in order for this chain to rotate, the π–π and electrostatic interactions in the chromophore assembly need to be overcome. Thus, molecules with longer chains above the chromophore can form ordered two-dimensional assemblies faster than those with shorter chains above the chromophore.

Several points emerge from the wetting studies. First, there is increasing disorder at the monolayer–air interface, for both the sulfones and the sulfides, as the length of the alkyl chain above the chromophore is reduced. Since this trend was observed for both the sulfones and the sulfides, and for all the liquids used to probe the surface, it seems likely that the phenomenon is mainly one of surface disorder rather than being due to the increasing influence of the dipole moment of the molecules on the probing droplet, as the length of alkyl chain between them was reduced. Second, on comparing the sulfides to their sulfone counterparts it was found that the sulfide monolayers gave higher contact angle values for almost all liquids used and that the hysteresis found for their water contact angles was smaller. From the total change in the contact angle, $\Delta\theta$, between having the shorter and the longer alkyl chains closer to the monolayer–air interface, one finds that for HD, the sulfides give $\Delta\theta \approx 5°$ while for the sulfones the change was larger, $\Delta\theta \approx 10°$. Since the HD contact angles primarily reflect changes in structural order rather than in electrostatic interactions, such a difference may be explained by poorer packing in the sulfone monolayers, either due to the bulkier SO_2 groups or possibly even to electrostatic repulsions between neighboring dipoles. For the water contact angles (advancing) the differences were larger with $\Delta\theta = 3°$ for the sulfides and $\Delta\theta = 12°$ for the sulfones. Although these results may be partly explained by increased disorder in the sulfone monolayers, it is possible, for monolayers formed from molecules of I, that the water may also be probing the larger dipolar forces associated with the sulfones.

The Zisman plots indicated that the monolayers formed from III and VI have surfaces most closely resembling those found for long-chain alkane thiols, i.e., $\gamma_c = 19$ mN m^{-1}.[7] As the alkyl chains above the chromophore are reduced in length, the critical surface tensions increase which is consistent with the picture that the order in the surface layer deteriorates to give a surface comprised of both methyl and methylene groups. However, the surfaces are still predominantly characteristic of a methyl rather than a methylene surface, and therefore structures *b* and *f* (Figure 12), which are expected to give surfaces with a large contribution of methylene groups, can be excluded. The value of γ_c found for monolayers of I is a little misleading, since this plot does not contain any angles from polar liquids. Using the Neumann "equation of state" or the method of splitting the surface energies into components, one finds that γ_{sv} is $\approx$3 mJ m^{-2} larger than γ_c (note, for molecules of III, VI, II, V, and IV the differences

(41) Hautman, J.; Klein, M. L. *J. Chem. Phys.* **1989**, *91*, 4994.
(42) Shnidman, Y.; Eilers, J. E.; Evans, S. D.; Ulman, A. In preparation.
(43) The 90% surface coverage value was not calculated from ψ and Δ values directly. This value was calculated on the basis of the average of the measured thickness. Thus, by comparing the amount of material in a uniform thin film of a specified thickness (i.e., measured value) to the fraction of the surface this would correspond to, if the same amount of material formed a thicker film (e.g., with the alkyl chains perpendicular to the surface).

Table V. Peak Widths (fwhm) for $\nu_s(CH_2)$, $\nu_s(CH_3)$, and $\nu_{as}(CH_3)$

monolayer	peak widths, cm^{-1}		
	$\nu_{as}(CH_3)$	$\nu_s(CH_3)^a$	$\nu_s(CH_2)$
I	18	8	10
II	7	7	11
III	7	7	11
IV	11	8	11
V	9	7	12
VI	5	6	8

[a] The $\nu_s(CH_3)$ stretch is split by a Fermi resonance (FR) interaction with a low-frequency CH_3 deformation. The fwhm values quoted here are for the stretch ca. 2878 cm^{-1}.

between γ_c and γ_{sv} are small). However, such differences are strongly dependent on which liquid is being used as a probe, for example, calculating γ_{sv} with the equation of state method yields 22.9 mJ m^{-2} with HD and 30.7 mJ m^{-2} with MI (for monolayers of I). Such discrepancies, however, also occur when the modified Fowkes-type equation is used though the differences are not so large. Thus, one is left with the problem that the surface energy measured seems to be a function of the liquid used to measure it. It is interesting, however, to note that the modified Fowkes equation yields the greatest polar contribution to the surface energy in the case of I for the sulfones and IV for the sulfides, i.e., what one would expect from the arguments of the position of the dipole with respect to the probing liquid. The perfluoro material VI(F) produced a very low energy surface γ_c = 9 mN m^{-1} which in comparison to PTFE and the perfluoroalkanoic acid on platinum suggests that the monolayer surfaces are mainly CF_3 in character. This is in marked contrast to results recently reported by Porter and Chau for perfluoroalkanoic acids on gold where it is clear that close-packed CF_3 surfaces are not formed.[44]

All the monolayers yield "crystalline-like" FTIR spectra with the amount of disorder within the films *increasing* as the chain length *above* the aromatic group decreases. Evidence for such increasing disorder in the FTIR spectra is 2-fold: first from the peak width measurements (fwhm) for the CH_3 and CH_2 stretches and second from the position of the C–H stretches for the monolayer compared to that obtained from the bulk materials (solution and KBr). Table V presents the results of these measurements for the symmetric stretches CH_2 and CH_3 at ca. 2850 and 2878 cm^{-1}, respectively, and for the CH_3 asymmetric stretch at 2966 cm^{-1}. The CH_2 asymmetric stretch is not used due to the difficulty in resolving it from the CH_3 symmetric Fermi resonance at 2936 cm^{-1}. In general it is found that the fwhm decrease with increasing chain length above the chromophore indicating a trend toward more "crystalline-like" monolayers. Furthermore it seems that the sulfides are more "crystalline-like" than their sulfone counterparts. The comparison of the peak positions between monolayer and bulk (solution and KBr) spectra indicates that the monolayers tend to be in a state closer to that found in the KBr (i.e., crystalline) rather than that found in the solution. Moving through each series, i.e., I–III and IV–VI, one finds that as the length of the upper alkyl chain is reduced the $\nu_{as}(CH_2)$ peak intensity changes significantly indicating a change in the molecular conformation. In particular it was noted that the integrated intensity of the $\nu_{as}(CH_2)$ and $\nu_s(CH_2)$ stretches was lowest in the case of molecules of II & V, i.e., with C_8 chains above and below the chromophore, and greatest for monolayers of I & IV. This would seem to imply that the degree of tilt in the monolayers in general follows the trend II,V < III,VI, < I,IV which is not the same order found for the surface disorder, estimated from the wetting results.

For the monolayers of II(D) the average orientations of the upper and lower alkyl chains, 47° and 51° tilt angles respectively, are slightly larger than found in previous studies for trichlorosilane monolayers containing similar chromophores.[3] The 40° tilt, 43° twist calculated for the monolayers of III is nearer to those generally found for alkane thiol monolayers on gold and gives an estimated thickness in close agreement with the ellipsometric measurements. The calculation of orientations from the transitions

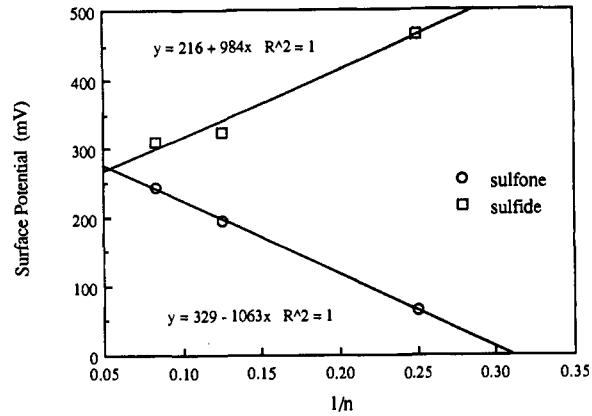

Figure 13. Surface potential vs $1/n$ (n = number of carbon atoms below the chromophore).

in the "mid-frequency" region is problematic since the values of $I_{obs}/3I_{cal}$ are greater than unity in some cases. Difficulties in obtaining reliable calculations for the sulfone vibrations arise due to the splitting of the asymmetric vibration and the overlap of several peaks. Furthermore, not only do the two asymmetric vibrations strongly overlap each other, they also overlap the aryl–O stretch close to 1260 cm^{-1}, added to which further difficulties may also arise due to overlap with the C–H wagging and twisting modes which can occur in this region. For the phenyl vibrations, ca. 1600–1500 cm^{-1}, the overlap between neighboring vibrations is quite small and does not really explain the large differences between the calculated and the observed spectra. Comparing the bulk spectra, of material II(D), for solid samples prepared in different ways i.e., from cast films, from KBr, and from the pure material (a powder crystallized from heptane, measured by diffused reflectance techniques), we found that the relative intensities of bands, in any given spectral region, can vary significantly from one form to the next. These variations are likely to be due to conformational and packing differences in the materials. In particular, we found that the KBr and the cast films differ significantly, and that the KBr spectra are most similar to those obtained from the pure material crystallized from heptane. Such differences in the "random" bulk spectra obtained from the different techniques cast doubt on the validity of using the KBr transmission spectra as a basis for computing the expected monolayer spectra, for the types of molecules studied here, especially in the "mid-frequency" region where the differences were the greatest.

The picture emerging from the surface potential results is consistent with the idea that the dipole associated with donor–acceptor group in the sulfones acts in the opposite direction to the net dipole found in the straight chain thiols (for the sulfides $\mu_{D-A\perp}$ acts in the same direction as that for the alkyl thiols).[24] The variation of the surface potential with chromophore position is slightly more difficult to explain. In the case of the sulfones it was found that the surface potential decreased as the distance between the gold surface and the chromophore was reduced (i.e., as the length of the aliphatic chain above the chromophore was increased). One of the possibilities which may explain such a variation in the surface potential, and the most plausible one, is that the dipole associated with the chromophore can be envisaged to have an image dipole located within the gold substrate at an equal distance from the surface and acting in the opposite direction. The electrostatic potential will be expected to vary inversely as a function of the separation, d, of the chromophore from the gold surface.[45] By plotting the values given in Table III as a function of the separation of the chromophore from the surface (Figure 13), it is found that the surface potential does vary like $1/d$ (the sulfones gave agreement better than should be expected) and thus the image dipole interpretation is also consistent with the observed behavior.[45,46]

(44) Porter, M.; Chau, L. *Chem. Phys. Lett.* **1990**, *167*, 198.

(45) A treatment of the "method of images" can be found in most electrostatics texts, for example, see: Knapp, A. G. *Surf. Sci.* **1973**, *34*, 289.

An alternative explanation, though one we feel is less likely, is that the observed trend in surface potential is a result of the changing order within the monolayers as the length of the alkyl chain above the chromophore is reduced. Increasing the amount of disorder within the monolayer could have two effects, it may either lead to a lower coverage of the gold surface by the monolayer, or it may alter the average orientation of the chromophores. Both of these phenomena could lead to the observed variations of a decreasing $\mu_\perp$ but there is no a priori reason why it should vary linearly, with the position of the chromophore in the alkyl chain, or that it should necessarily decrease in size. The thickness determinations of the monolayers would seem to suggest that coverage is more or less constant for all the monolayers and thus the argument of fractional coverage does not really seem very persuasive. It is noted however, that due to the size of the chromophore dipole only small changes in its orientation could have a significant effect on the observed surface potential.

Similarly the behavior of the sulfides may also be explained as being due to either the image-dipole interpretation (in this case the contact potential decreases as the chromophore is moved further away from the substrate since the dipole associated with the chromophore acts in the opposite direction than found for the sulfones)[47] or the orientation changes of the chromophore. So, although the surface potential results give easily understandable information on the effects of incorporating a dipole into an otherwise straight-chain molecule, they also lead to some interesting, if not fully understandable, results regarding the effects of the position of the chromophore in the monolayer. Such insights into the effects of varying the chromophore position on the surface potential may be of interest in the use of monolayers for modifying the work functions of surfaces and in understanding electron-transfer processes at surfaces.

Monolayers of VI(F) gave large negative changes in the surface potential. Such results are expected due to the strong electron withdrawing fluoro groups. For the molecules in these monolayers, the net dipole acts in the opposite direction to those found for monolayers of I–VI, and these monolayers may therefore be represented as a dipole sheet in which a sheet of positive charges resides close to the substrate surface and a sheet of negative charges resides toward the monolayer–air interface. Such an arrangement clearly indicates that the effect of the perfluoro-monolayer is to increase the work function of the gold. This result is in agreement with the results reported by Chidsey and Loiacono for electron tunnelling through various thiol monolayers, in which they report that the barrier for electron tunnelling clearly increases in going from the alkane thiols to perfluoroalkane thiols.[48,49]

Differences were found to emerge from the wetting data, if the aromatic group was displaced by one carbon in its chain position $(CH_3-(CH_2)_{10}-SO_2-Ph-O-(CH_2)_5-SH$, VII, compared to $CH_3-(CH_2)_{11}-SO_2-Ph-O-(CH_2)_4-SH$, III, Table I). These can be readily explained in terms of the degree of molecular tilt or disorder introduced into the monolayer by this displacement. The reason why such a subtle change in the chromophore position should display so dramatic an effect on the monolayer quality is not certain; however, its effects are clearly seen on comparing the reflection–absorption spectra of III and VII. Figure 9 shows an increase in the peak areas for the CH_2 stretches in the "high-frequency" region for monolayers of VII over those of III; further the asymmetric CH_3 stretch is also increased while its symmetric counterpart is decreased. Such changes are indicative of increasing molecular tilt (or disorder) in monolayers of VII. As the tilt in the monolayers increases the composition of the surface changes with there being increasing contributions from methylene groups

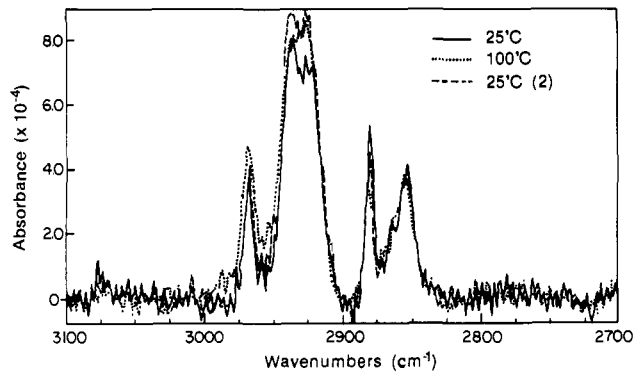

Figure 14. The variation of the high-frequency IR spectrum for a monolayer of II as a function of temperature.

thus increasing the free energy of the surface. Changes in the "mid-frequency" region are also supportive of this interpretation, where it is found that the phenyl vibrations decrease in intensity (for monolayers of VII) as the tilt the phenyl vibration makes with the surface normal is increased. Finally from ellipsometry it was found that monolayers VII gave lower thicknesses ≈21 Å which could also be indicative of increasing tilt. From Figure 12 it can be seen that structures such as *e* and *f* may be in agreement with the measured thickness. However, it is only structure *f* that can explain both the thickness and wetting results. That structure *f* does indeed represent the actual molecular orientation in the monolayer is not clear. It does, however, emphasize the fact that the packing and orientation of amphiphiles having such complex structures is not at all trivial.

The thermal stability of monolayers was monitored by looking at the IR spectra as a function of temperature. The monolayers were heated in 20 °C steps from room temperature to between 100 and 120 °C and allowed to equilibrate at each temperature for 20 min before spectra were taken. It was found that all monolayers showed some increase in tilt or disorder following the heating process; however, this was smallest for monolayers of III and VI and increased with decreasing chain length above the aromatic group. The example spectra (Figure 14) shows the results of heating a monolayer of II to 100 °C and the changes found on returning to room temperature. It is evident that there is some decrease in order within this monolayer, which is also seen by the slight decrease in the contact angles found for the subsequent Zisman plots.[50] Such changes are, however, only relatively small and indicate that the monolayers are robust.

The silver was "over" deposited for the SERS study of these monolayers because of problems previously experienced when attempting to form a self-assembled monolayer of materials with SH head groups on a roughened silver substrate.[40] Although the layer appeared to form on the roughened silver, no SERS scattering was observed.[51] We believe that the thiol reacts with the silver substrate to form a silver sulfide at the metal surface and that the silver sulfide is no longer effective in supporting SER scattering. In defense of our current approach, it was demonstrated that silver islands can be successfully deposited onto evaporated organic films and Langmuir–Blodgett monolayers to enhance the Raman scattering from these structures without changing the character of the films.[52]

In all of the monolayers studied here, the predominant features observed are associated with the aromatic ring and nearby functionalities (e.g., SO_2). Selective mode enhancement resulting from unique interactions between the enhancing metal and the observed structure have been reported for a variety of materials.[53]

(46) The separation between the chromophore and the surface is arbitrarily taken to be the number of alkyl groups below the chromophore.

(47) Calculations from MOPAC do indicate that the dipoles of the sulfones and sulfides act in opposite directions, see Figure 1.

(48) Chidsey, C. D.; Loiacono, D. N. *Langmuir* **1990**, *6*, 682.

(49) While we note that Chidsey interprets his results as being due to the blocking of the acceptors reaching the gold electrodes, such an interpretation is note required from our experiments and as such are totally explainable by simple electrostatics.

(50) On some occasions such heating led to surfaces with lower critical surface tensions indicating that there may be some annealing of defects within the monolayers.

(51) Ferris, N. S.; Ulman, A. Unpublished observations.

(52) (a) Ferris, N. S.; Littman, J. E. *SPIE Proc.* **1989**, *1055*, 117. (b) Ferris, N. S.; Penner, T. Manuscript in preparation.

(53) Chang, R. K.; Furtak, E., Eds. *Surface Enhanced Raman Scattering*; Plenum Press: New York, 1982.

We consider our observations to indicate a propensity of the over deposited silver to associate with these specific functionalities in the monolayers. In addition, we observe a wide variation in the S–N ratio among the SERS spectra of the monolayers as the aliphatic tails are lengthened from four to twelve carbons (Figure 10). The distance dependence of the SERS enhancement is documented for thin multilayered films.[54] In the present study, it appears that the aliphatic tails may act as barriers to the penetration of silver into the monolayer. The longer the tail (four to twelve carbons) the farther the silver will be from the aromatic ring and the less effective it will be in enhancing the Raman scattering. In fact, for the C_{12} structure almost no Raman scattering is observed, possibly because the aromatic ring is buried at a distance from the silver that is beyond the effective enhancement range. The Raman scattering from the C_8 structures is relatively strong and may result from either significant penetration of the metal into the layer, or from a shortened distance of the aromatic ring to the surface because of the tilting of the aliphatic tail. During the course of the experiments we did observe that some monolayers appeared to be sensitive to the power level of the incident radiation. Figure 11 shows a comparison of results of short, successive integrations of the SERS signal from monolayers of II (C_8SO_2) and V (C_8S). On the time scale of these collections, the C_8SO_2 monolayer is stable in the laser beam. In contrast, the spectrum of the C_8 film shows significant changes in the $\sim$1100-cm^{-1} region. We believe that the loss in intensity of the 1092-cm^{-1} band and the growth of the 1078-cm^{-1} band may be associated with a photoinduced, metal-mediated oxidation of the sulfide to a sulfinyl (–S- to –S=O). These mid-frequency region changes are accompanied by a loss in intensity in the $\sim$600-cm^{-1} region associated with the C–S stretching motion of the molecule. The instability toward oxidation of the sulfide structure is a likely result of the combination of high power densities and the presence of the metal.

Conclusions

This study has shown that it is possible to incorporate aromatic groups with large net dipole moments into monolayers, without adversely affecting the quality of the monolayers formed. One condition necessary for the formation of monolayers with well-ordered surfaces is that the aliphatic chain above the aromatic group, i.e., at the monolayer–air interface, should be greater than C_8 in length, with the best results being found for C_{12}-chains above the aromatic group. Since the chain between the aromatic group and the gold surface seems to have little effect on the monolayer–air surface this portion of the chain may be kept to a minimum so as not to "dilute" the effect of the chromophore for application purposes.

Further, it was found that the films containing the bulkier, more polar sulfone groups were less ordered than their sulfide counterparts.

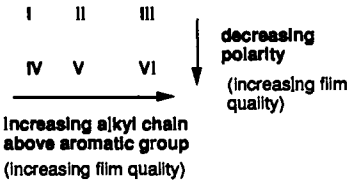

This would appear to suggest that there may be a limit to either the size or the strength of the polar aromatic group being introduced before the disorder in the monolayer becomes too great. Despite the fact that no unique conclusions can be drawn on the average orientation of the molecules within these monolayers, evidence from wetting (e.g., large HD contact angles) and FTIR (large $\nu_s(CH_3)/\nu_{as}(CH_3)$ ratio) suggest that structures similar to *c* and *d* shown in Figure 12 are most likely.

A further important fact to emerge from these studies is that even slight changes in position of the aromatic group in the alkyl chain may strongly effect both the monolayer surface produced and the orientation of the chromophore (and hence the direction of its dipole moment) and must therefore be considered in the building of multilayer films for NLO applications or in the engineering of surfaces.

Acknowledgment. We thank Professor R. H. Tredgold of the Physics Department, University of Lancaster, UK, for a valuable discussion of the surface potential results and V. DePalma for the use of the surface potential apparatus. Our thanks are also due to T. Penner and J. Schildkraut for useful discussions of the results and to D. E. Margevich and D. J. Motyl for the measurement of bulk IR spectra for these materials, all of Eastman Kodak Company. Finally we acknowledge M. Porter, of the Chemistry Department, University of Iowa, for providing bulk refractive index constants of ODT to help in checking the correct working of our program for computing the molecular orientation information.

Supplementary Material Available: Details of the preparation of compounds I–VII, II(D), and VI(F) (6 pages). Ordering information is given on any current masthead page.

(54) Murray, C. A.; Allara, D. A. *J. Phys. Chem.* **1982**, *76*, 1290.